



# Mathematical modelling of PV array under partial shading condition

VANDANA JHA

Department of Electrical Engineering, C.V. Raman Global University, Bhubaneswar 752054, India  
e-mail: vandana.jha.electrical@gmail.com

MS received 5 January 2022; revised 16 February 2022; accepted 23 February 2022

**Abstract.** This paper proposes mathematical modelling of photovoltaic (PV) array under partial shading condition. The proposed mathematical modelling is capable of predicting the output characteristics of PV array of any dimension, made of any kind of PV modules, having any number of bypass diodes, and for any shading pattern (irradiance and temperature) by utilizing only the values of the parameters of PV module provided in the manufacturer's datasheets. Although the proposed modelling can be implemented by any software tool, in this paper, it has been implemented using MATLAB programming. The proposed modelling has been validated on two PV arrays ((i) PV array made of four WS-330 PV modules configured in SP configuration and (ii) PV array made of four HSTBF24265P PV modules configured in TCT configuration) for in total of five test cases to establish its robustness. The test cases cover situations ranging from the most probable to least probable shading scenarios. The results generated by MATLAB programming of the proposed equations of PV array under uniform irradiance condition and partial shading condition have been validated by the results obtained by MATLAB simulation. The proposed modelling has also been experimentally validated on the aforementioned PV arrays.

**Keywords.** PV module; PV array; modelling; partial shading condition; bypass diodes; MATLAB.

## 1. Introduction

The exhaustible nature of non-renewable energy sources, rising concern over environmental problems such as global warming, and overall energy emergency are the vital inspirations behind the growing exploitation of renewable energy sources. Among various non-conventional energy sources, solar energy (Photovoltaics), as a consequence of improved solar cell manufacturing proficiency, cost reduction, and progress in conversion technology, has experienced wide popularity for electricity generation around the world [1]. In several implementations, photovoltaic (PV) systems are being progressively employed as they have many attractive characteristics such as maintenance freedom, low weight and function cost, modularity, and eco-friendliness [2, 3]. On the other hand, trouble in treatment of the nonlinear output characteristic of a PV source, which varies with environmental conditions (temperature and solar irradiance), is the main disadvantage of its employment [4, 5]. The problem in handling the output characteristics of a PV source rises manifold when some portions of its surface get shaded, resulting in the fact that the whole PV source could not receive uniform irradiance and temperature. This condition is known as the partial shading condition (PSC). Partial shading is the most significant issue leading to mismatch losses which can

minimize the output power of a PV system to a considerable extent [6, 7].

Many researchers have analyzed the effects of partial shading on PV systems [8, 9]. Partial shading can be caused by various things such as stationary or moving clouds, neighbouring buildings and trees, birds and bird litters, or snow covering the surface of PV sources [10]. The shaded string of PV cells or modules may get reverse biased due to which they start acting as an external load consuming the power generated by other solar cells or modules. This will eventually decrease the output power of PV modules or arrays. In extreme conditions, the probability of occurrence of the hot-spot phenomena appears, which can lead to permanent damage of cells or modules [11]. To protect the system against hot-spot damage, to minimize mismatch effects, and to reduce the decrease of power generation, all of which originate due to partial shading, the most reasonable solution is to incorporate a bypass diode across a string of PV cells or module [12, 13]. Utilizing bypass diodes results in the multi-peak power-voltage characteristic of a PV module or array under PSC [14].

This paper proposes mathematical modelling of PV array under PSC. The proposed modelling, which can be implemented by any software tool, utilizes only the values of the parameters of the PV module mentioned in the datasheets

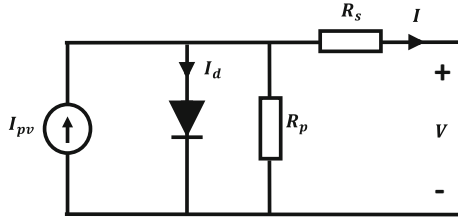


**Figure 1.** Single-diode equivalent circuit of a PV module.

given by the manufacturers and can accurately determine the output characteristics of PV array of any dimension, made of any kind (type and manufacturer) of PV modules, having any number of bypass diodes, and for any environmental condition (irradiance and temperature).

## 2. Mathematical modelling of PV module

Figure 1 shows the single-diode equivalent circuit of a PV module.

The arithmetical expression which describes the  $I - V$  characteristic of a PV module is

$$I = I_{pv} - I_o \left[ \exp\left(\frac{V + R_s I}{V_t a}\right) - 1 \right] - \left(\frac{V + R_s I}{R_p}\right) \quad (1)$$

$$V_t = N_s k T / q \quad (2)$$

Since the value of  $R_p$  is usually very high, therefore,  $\left(\frac{V + R_s I}{R_p}\right)$  term of the eq. (1) can be approximated to zero.

$$I = \frac{G}{G_{STC}} \left( I_{scSTC} + K_{I_{sc}}^T \Delta T \right) - \left( \frac{\frac{G}{G_{STC}} \left( I_{scSTC} + K_{I_{sc}}^T \Delta T \right)}{\left[ \exp\left(\frac{(1 + K_{V_{oc}}^G (\log(G/G_{STC}))) (V_{ocSTC} + K_{V_{oc}}^T \Delta T)}{V_t a}\right) - 1 \right]} \right) \left[ \exp\left(\frac{V + R_s I}{V_t a}\right) - 1 \right] \quad (11)$$

$$\left(\frac{V + R_s I}{R_p}\right) \approx 0 \quad (3)$$

From eqs. (1) and (3), eqs. (4) and (5) are obtained.

$$I = I_{pv} - I_o \left[ \exp\left(\frac{V + R_s I}{V_t a}\right) - 1 \right] \quad (4)$$

$$V = V_t a \ln\left(\frac{I_{pv} - I + I_o}{I_o}\right) - R_s I \quad (5)$$

The  $V_{oc}$  and  $I_{sc}$  of a PV module depend on both solar irradiance and temperature and can be expressed as [15]

$$V_{oc} = \left(1 + K_{V_{oc}}^G (\log(G/G_{STC}))\right) \left(V_{ocSTC} + K_{V_{oc}}^T \Delta T\right) \quad (6)$$

$$I_{sc} = \frac{G}{G_{STC}} \left(I_{scSTC} + K_{I_{sc}}^T \Delta T\right) \quad (7)$$

The  $I_{pv}$  of a PV module is approximately equal to the  $I_{sc}$  at any environmental condition [15]. The  $I_{pv}$  of a PV module can be expressed as

$$I_{pv} \approx I_{sc} = \frac{G}{G_{STC}} \left(I_{scSTC} + K_{I_{sc}}^T \Delta T\right) \quad (8)$$

The  $I_o$  of a PV module can be expressed as [15]

$$I_o = \frac{I_{pv}}{\left[\exp\left(\frac{V_{oc}}{V_t a}\right) - 1\right]} \quad (9)$$

Substituting eqs. (6) and (8) in eq. (9), eq. (10) is obtained.

$$I_o = \frac{\frac{G}{G_{STC}} \left(I_{scSTC} + K_{I_{sc}}^T \Delta T\right)}{\left[\exp\left(\frac{(1 + K_{V_{oc}}^G (\log(G/G_{STC}))) (V_{ocSTC} + K_{V_{oc}}^T \Delta T)}{V_t a}\right) - 1\right]} \quad (10)$$

Substituting eqs. (8) and (10) in eq. (4), eq. (11) is obtained.

Substituting eqs. (8) and (10) in eq. (5), eq. (12) is obtained.

$$I_{12} = I_1 \text{ or } I_2 \tag{14}$$

$$V_1' = \text{interpolation}(I_1, V_1, I_2) \tag{15}$$

$$V = V_t \ln \left( \frac{\left( \frac{G}{G_{STC}} (I_{sc,STC} + K_{I_{sc}}^T \Delta T) - I + \left( \frac{\frac{G}{G_{STC}} (I_{sc,STC} + K_{I_{sc}}^T \Delta T)}{\left[ \exp \left( \frac{(1+K_{V_{oc}}^G (\log(G/G_{STC})) (V_{oc,STC} + K_{V_{oc}}^T \Delta T)}{V_{t,a}}) - 1 \right]} \right)} \right)}{\left( \frac{\frac{G}{G_{STC}} (I_{sc,STC} + K_{I_{sc}}^T \Delta T)}{\left[ \exp \left( \frac{(1+K_{V_{oc}}^G (\log(G/G_{STC})) (V_{oc,STC} + K_{V_{oc}}^T \Delta T)}{V_{t,a}}) - 1 \right]} \right)} \right)} \right) - R_s I \tag{12}$$

### 3. Mathematical modelling of PV array under partial shading condition

A PV array is formed by connecting PV modules in different configurations.

#### 3.1 Mathematical modelling of series-parallel PV array configuration

Figure 2 shows the schematic diagram of a PV array in which four PV modules are connected in series-parallel (SP) configuration. It is assumed that the bypass diode is connected across each module.

By utilizing eq. (12) in figure 2, it can be written that Similarly,  $V_2$ ,  $V_3$ , and  $V_4$  are obtained.

Referring to figure 2, it can be noticed that module 1 and module 2 are connected in series. Therefore, the current

$$V_2' = \text{interpolation}(I_2, V_2, I_2) \tag{16}$$

$$V_{12} = V_1' + V_2' \tag{17}$$

Similarly, it can be noticed that module 3 and module 4 are connected in series. Therefore, the current flowing through module 3 and module 4 is equal and the respective voltages across module 3 and module 4 are added.

$$I_{34} = I_3 \text{ or } I_4 \tag{18}$$

$$V_3' = \text{interpolation}(I_3, V_3, I_{34}) \tag{19}$$

$$V_4' = \text{interpolation}(I_4, V_4, I_{34}) \tag{20}$$

$$V_{34} = V_3' + V_4' \tag{21}$$

$$V_1 = \left( V_{t1} \ln \left( \frac{\left( \frac{G_1}{G_{STC}} (I_{sc,STC} + K_{I_{sc}}^T \Delta T_1) - I_1 + \left( \frac{\frac{G_1}{G_{STC}} (I_{sc,STC} + K_{I_{sc}}^T \Delta T_1)}{\left[ \exp \left( \frac{(1+K_{V_{oc}}^G (\log(G_1/G_{STC})) (V_{oc,STC} + K_{V_{oc}}^T \Delta T_1)}{V_{t1,a}}) - 1 \right]} \right)} \right)}{\left( \frac{\frac{G_1}{G_{STC}} (I_{sc,STC} + K_{I_{sc}}^T \Delta T_1)}{\left[ \exp \left( \frac{(1+K_{V_{oc}}^G (\log(G_1/G_{STC})) (V_{oc,STC} + K_{V_{oc}}^T \Delta T_1)}{V_{t1,a}}) - 1 \right]} \right)} \right)} \right) - R_s I_1 \tag{13}$$

flowing through module 1 and module 2 is equal and the respective voltages across module 1 and module 2 are added.

By utilizing eq. (11) in figure 2, it can be written that

$$I_{12} = \left( \frac{G_{12}}{G_{STC}} (I_{scSTC} + K_{I_{sc}}^T \Delta T_{12}) - \left( \frac{\frac{G_{12}}{G_{STC}} (I_{scSTC} + K_{I_{sc}}^T \Delta T_{12})}{\left[ \exp \left( \frac{(1+K_{V_{oc}}^G (\log(G_{12}/G_{STC})) (V_{ocSTC} + K_{V_{oc}}^T \Delta T_{12}))}{V_{112} a} \right) - 1 \right]} \right) \left[ \exp \left( \frac{V_{12} + R_s I_{12}}{V_{112} a} \right) - 1 \right] \right) \quad (22)$$

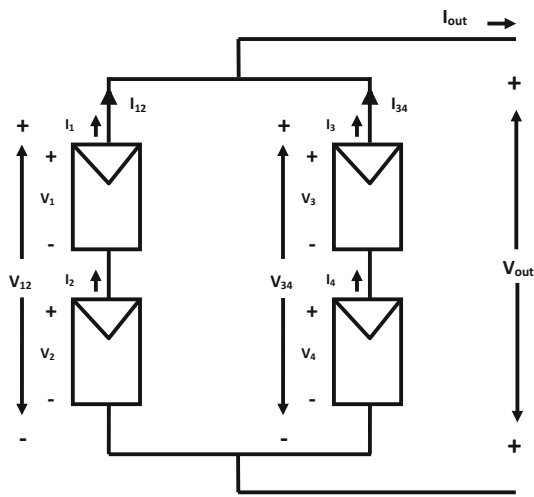


**Figure 2.** Schematic diagram of a PV array connected in SP configuration.

Similarly,  $I_{34}$  is obtained.

Referring to figure 2, it can be noticed that branch 12 and branch 34 are connected in parallel. Therefore, the voltage across branch 12 and branch 34 is equal and the respective currents flowing through branch 12 and branch 34 are added.

$$V_{out} = V_{12} \text{ or } V_{34} \quad (23)$$

$$I_{12}' = \text{interpolation}(V_{12}, I_{12}, V_{out}) \quad (24)$$

$$I_{34}' = \text{interpolation}(V_{34}, I_{34}, V_{out}) \quad (25)$$

$$I_{out} = I_{12}' + I_{34}' \quad (26)$$

### 3.2 Mathematical modelling of total-cross-tied PV array configuration

Figure 3 shows the schematic diagram of a PV array in which four PV modules are connected in total-cross-tied (TCT) configuration. It is assumed that the bypass diode is connected across each module.

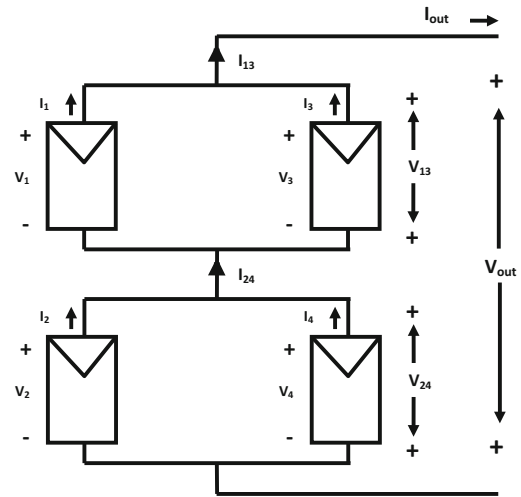


**Figure 3.** Schematic diagram of a PV array connected in TCT configuration.

**Table 1.** Specifications of WS-330 and HSTBF24265P PV modules at STC.

Parameters	WS-330 PV module	HSTBF24265P PV module
$P_{mpp}$ (W)	330	265
$V_{mpp}$ (V)	37.95	36.0
$I_{mpp}$ (A)	8.70	7.36
$V_{oc}$ (V)	46.70	43.70
$I_{sc}$ (A)	9.25	7.93
$K_{V_{oc}}^T$ (%/°C)	- 0.2627	- 0.27
$K_{I_{sc}}^T$ (%/°C)	0.0118	0.04
$N_s$	72	60

By utilizing eq. (11) in figure 3, it can be written that

$$I_1 = \left( \frac{G_1}{G_{STC}} (I_{scSTC} + K_{I_{sc}}^T \Delta T_1) - \left( \frac{\frac{G_1}{G_{STC}} (I_{scSTC} + K_{I_{sc}}^T \Delta T_1)}{\left[ \exp \left( \frac{(1+K_{V_{oc}}^G (\log(G_1/G_{STC})))(V_{ocSTC} + K_{V_{oc}}^T \Delta T_1)}{V_{i1}a} \right) - 1 \right]} \right) \right) \left[ \exp \left( \frac{V_1 + R_s I_1}{V_{i1}a} \right) - 1 \right] \quad (27)$$

Similarly,  $I_2$ ,  $I_3$ , and  $I_4$  are obtained.

Referring to figure 3, it can be noticed that module 1 and module 3 are connected in parallel. Therefore, the voltage across module 1 and module 3 is equal and the respective currents flowing through module 1 and module 3 are added.

$$V_{13} = V_1 \text{ or } V_3 \quad (28)$$

$$I_1' = interpolation(V_1, I_1, V_{13}) \quad (29)$$

$$I_3' = interpolation(V_3, I_3, V_{13}) \quad (30)$$

$$I_{13} = I_1' + I_3' \quad (31)$$

Similarly, it can be noticed that module 2 and module 4 are connected in parallel. Therefore, the voltage across module 2 and module 4 is equal and the respective currents flowing through module 2 and module 4 are added.

$$V_{24} = V_2 \text{ or } V_4 \quad (32)$$

$$I_2' = interpolation(V_2, I_2, V_{24}) \quad (33)$$

$$I_4' = interpolation(V_4, I_4, V_{24}) \quad (34)$$

$$I_{24} = I_2' + I_4' \quad (35)$$

By utilizing eq. (12) in figure 3, it can be written that

Referring to figure 3, it can be noticed that branch 13 and branch 24 are connected in series. Therefore, the current flowing through branch 13 and branch 24 is equal and the respective voltages across branch 13 and branch 24 are added.

$$I_{out} = I_{13} \text{ or } I_{24} \quad (37)$$

$$V_{13}' = interpolation(I_{13}, V_{13}, I_{out}) \quad (38)$$

$$V_{24}' = interpolation(I_{24}, V_{24}, I_{out}) \quad (39)$$

$$V_{out} = V_{13}' + V_{24}' \quad (40)$$

#### 4. Validation of the proposed modelling of PV array

The WS-330 and HSTBF24265P PV modules have been considered for validation of the proposed modelling. The specifications of WS-330 and HSTBF24265P PV modules at standard test condition (STC) are given in table 1.

The proposed modelling (which executes numerical evaluation of the PV model) is encoded in MATLAB programming for all the test cases considered in this paper. The proposed modelling is validated on

$$V_{13} = \left( V_{i13} a \ln \left( \frac{\frac{G_{13}}{G_{STC}} (I_{scSTC} + K_{I_{sc}}^T \Delta T_{13}) - I_{13} + \left( \frac{\frac{G_{13}}{G_{STC}} (I_{scSTC} + K_{I_{sc}}^T \Delta T_{13})}{\left[ \exp \left( \frac{(1+K_{V_{oc}}^G (\log(G_{13}/G_{STC})))(V_{ocSTC} + K_{V_{oc}}^T \Delta T_{13})}{V_{i13}a} \right) - 1 \right]} \right)}{\left( \frac{\frac{G_{13}}{G_{STC}} (I_{scSTC} + K_{I_{sc}}^T \Delta T_{13})}{\left[ \exp \left( \frac{(1+K_{V_{oc}}^G (\log(G_{13}/G_{STC})))(V_{ocSTC} + K_{V_{oc}}^T \Delta T_{13})}{V_{i13}a} \right) - 1 \right]} \right)}} \right) - R_s I_{13} \right) \quad (36)$$

Similarly,  $V_{24}$  is obtained.

**(i) PV array-1:** PV array-1 is made of four WS-330 PV modules configured in SP configuration.

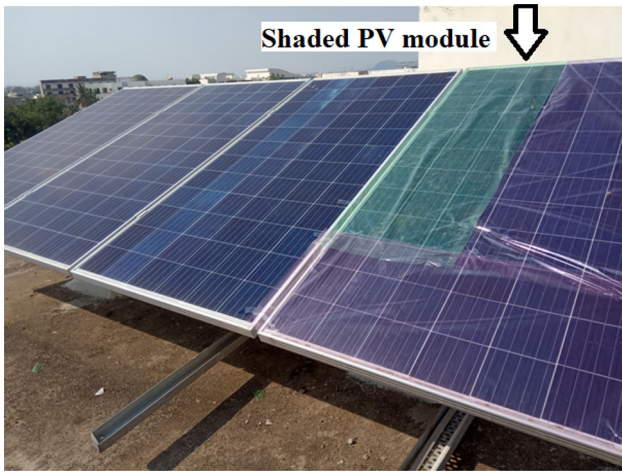


**Figure 4.** Real PV array-1 utilized for the experimental validation of proposed modelling.

(ii) **PV array-2:** PV array-2 is made of four HSTBF24265P PV modules configured in TCT configuration.

Following test cases have been considered for the validation of the proposed modelling:

**Case-1:** For case-1, the proposed modelling is validated on a real PV array-1 as shown in figure 4. The PV modules forming PV array-1 are mounted on the terrace of C.V. Raman Global University, India. The experiment was conducted on 02 Feb 2022 and the readings of irradiance and temperature at 12:25:08 PM were recorded as 709 W/m<sup>2</sup> and 31°C respectively. For validation, one PV module was covered with transparent coloured paper to produce the partial shading effect. The proposed modelling has been executed for the referred condition on PV array-1. The results produced by the proposed modelling (which evaluates the PV model numerically) are compared with the results generated by the MATLAB/SIMULINK and experimental method. The comparison of the results obtained from numerical evaluation and simulation of the PV model for case-1 is shown in table 2. The  $P - V$

characteristics generated by the proposed modelling are depicted with the experimental points for case-1 in figure 5.

**Case-2:** For case-2, the proposed modelling is validated on a real PV array-2 as shown in figure 6. The PV modules forming PV array-2 are mounted on another terrace of C.V. Raman Global University, India. The experiment was conducted on 12 Feb 2022 and the readings of irradiance and temperature at 1:40:08 PM were recorded as 697 W/m<sup>2</sup> and 28°C respectively. For validation, one PV module was covered with transparent coloured paper to produce the partial shading effect. The comparison of the results obtained from numerical evaluation and simulation of the PV model for case-2 is shown in table 3. The  $P - V$  characteristics generated by the proposed modelling are depicted with the experimental points for case-2 in figure 7.

**Case-3:** For case-3, the most probable shading scenario representing objective shading (shading caused due to environmental conditions) has been considered on both PV array-1 and PV array-2. The irradiance received by each module is taken as 650 W/m<sup>2</sup>, 700 W/m<sup>2</sup>, 750 W/m<sup>2</sup>, and 800 W/m<sup>2</sup> respectively. The irradiance received by PV modules has been considered more or less equal which justifies the scenario of objective shading. The comparison of the results obtained from numerical evaluation and simulation of the PV model for case-3 is shown in table 4.

**Case-4:** For case-4, the most probable shading scenario representing subjective shading (shading caused due to an oddity in the vicinity of a PV system) has been considered on both PV array-1 and PV array-2. The irradiance received by each module is taken as 400 W/m<sup>2</sup>, 450 W/m<sup>2</sup>, 800 W/m<sup>2</sup>, and 800 W/m<sup>2</sup> respectively. The irradiance received by two PV modules, which are perceived to be shaded, has been considered low in comparison to other modules. This justifies the scenario of subjective shading. The comparison of the results obtained from numerical evaluation and simulation of the PV model for case-4 is shown in table 5.

**Case-5:** For case-5, the least probable shading scenario representing arbitrary shading (shading scenario which is unrealistic) has been considered on both PV array-1 and PV array-2. The irradiance received by each module is taken as

**Table 2.** Comparison of results obtained from numerical evaluation and simulation of the PV model for case-1.

Condition	Parameters	Numerical evaluation of the PV model	Simulation of the PV model	Absolute error (%)
Uniform irradiance condition	$P_{MPP}$ (W)	940.5443	928.3469	1.2968
	$V_{MPP}$ (V)	75.1353	75.0936	0.0555
	$I_{MPP}$ (A)	12.5180	12.3625	1.2422
	$V_{OC}$ (V)	90.7604	90.5980	0.1789
	$I_{SC}$ (A)	13.1258	13.1444	0.1417
Partial shading condition	$P_{MPP}$ (W)	792.3665	783.0024	1.1818
	$V_{MPP}$ (V)	76.4854	76.7748	0.3784
	$I_{MPP}$ (A)	10.3597	10.1987	1.5541
	$V_{OC}$ (V)	90.7604	90.4112	0.3847
	$I_{SC}$ (A)	13.1258	13.1443	0.1409



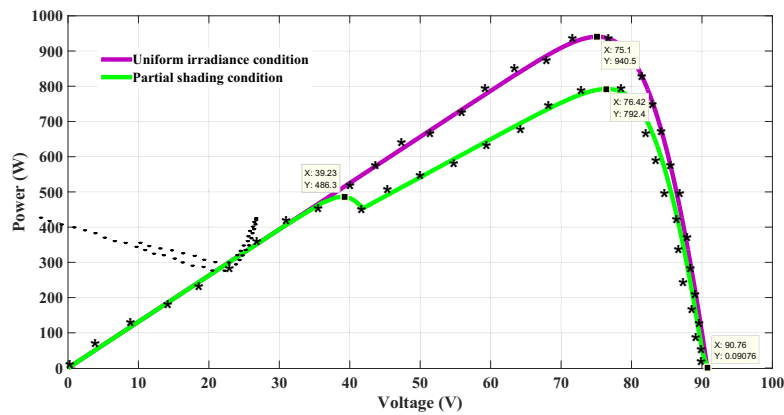


Figure 5.  $P - V$  characteristics generated by proposed modelling depicted with the experimental points for case-1.



Figure 6. Real PV array-2 utilized for the experimental validation of proposed modelling.

325  $W/m^2$ , 542  $W/m^2$ , 776  $W/m^2$ , and 964  $W/m^2$  respectively. There is a very sharp difference in the irradiance received by adjacent PV modules which is very unlikely to happen in reality. This justifies the scenario of arbitrary

shading. The comparison of the results obtained from numerical evaluation and simulation of the PV model for case-5 is shown in table 6.

It can be observed from tables 2, 3, 4, 5 and 6, that there is a very small percentage error between the results obtained from the numerical evaluation (proposed modelling) and simulation of the PV model which validates the proposed modelling theoretically. Ideally, there should not be any error but still, the small error exists because in the proposed modelling,  $R_p$  has been neglected (as it is evident in section 2) and in the simulation model,  $R_p$  has been taken into consideration.

From figure 5 and figure 7, it can be noticed that almost all the experimental points are aligned with the curve generated by the proposed modelling. Thus, the proposed modelling is experimentally validated.

### 5. Conclusion

In this paper, mathematical modelling of PV array under partial shading condition has been proposed. The proposed modelling is competent in forecasting the output of PV array of any dimension, made of any kind (type and

Table 3. Comparison of results obtained from numerical evaluation and simulation of the PV model for case-2.

Condition	Parameters	Numerical evaluation of the PV model	Simulation of the PV model	Absolute Error (%)
Uniform irradiance condition	$P_{MPP}$ (W)	757.4659	737.3874	2.6507
	$V_{MPP}$ (V)	71.6619	71.6680	0.0085
	$I_{MPP}$ (A)	10.5700	10.2889	2.6594
	$V_{OC}$ (V)	85.5404	85.4772	0.0739
	$I_{SC}$ (A)	11.0677	11.0932	0.2304
Partial shading condition	$P_{MPP}$ (W)	663.0689	645.7643	2.6098
	$V_{MPP}$ (V)	73.2026	73.2412	0.0527
	$I_{MPP}$ (A)	9.0580	8.8170	2.6606
	$V_{OC}$ (V)	85.5398	85.1276	0.4819
	$I_{SC}$ (A)	11.0677	11.0928	0.2268

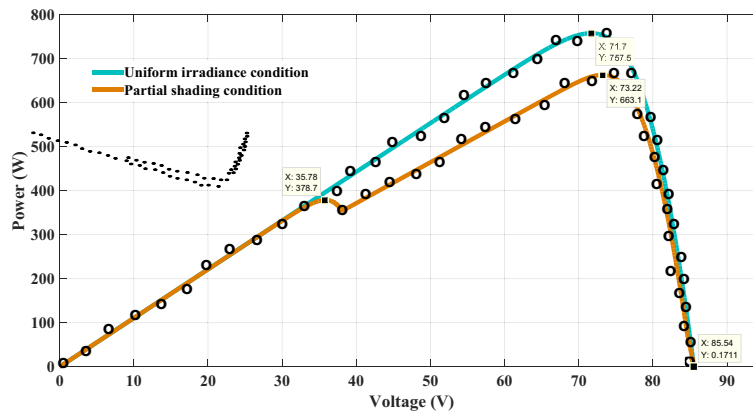


Figure 7.  $P - V$  characteristics generated by proposed modelling depicted with the experimental points for case-2.

Table 4. Comparison of results obtained from numerical evaluation and simulation of the PV model for case-3.

Parameters	PV array-1			PV array-2		
	Numerical evaluation of the PV model	Simulation of the PV model	Absolute Error (%)	Numerical evaluation of the PV model	Simulation of the PV model	Absolute Error (%)
$P_{MPP}$ (W)	971.4240	958.6800	1.3119	786.7003	765.7120	2.6679
$V_{MPP}$ (V)	77.2483	77.1484	0.1293	72.9509	72.8916	0.0813
$I_{MPP}$ (A)	12.5753	12.4264	1.1841	10.7840	10.5048	2.5890
$V_{OC}$ (V)	92.5498	92.4660	0.0905	86.5929	86.3512	0.2791
$I_{SC}$ (A)	13.8750	13.8944	0.1398	11.8950	11.9220	0.2270

Table 5. Comparison of results obtained from numerical evaluation and simulation of the PV model for case-4.

Parameters	PV array-1			PV array-2		
	Numerical evaluation of the PV model	Simulation of the PV model	Absolute Error (%)	Numerical evaluation of the PV model	Simulation of the PV model	Absolute Error (%)
$P_{MPP}$ (W)	820.9276	810.1598	1.3117	668.6157	650.7459	2.6727
$V_{MPP}$ (V)	77.0983	77.1484	0.0650	72.5725	72.5420	0.0420
$I_{MPP}$ (A)	10.6478	10.5013	1.3759	9.2131	8.9706	2.6321
$V_{OC}$ (V)	92.6570	91.7188	1.0126	86.6947	85.8268	1.0011
$I_{SC}$ (A)	11.5625	11.5788	0.1410	9.9125	9.9350	0.2270

Table 6. Comparison of results obtained from numerical evaluation and simulation of the PV model for case-5.

Parameters	PV array-1			PV array-2		
	Numerical evaluation of the PV model	Simulation of the PV model	Absolute error (%)	Numerical evaluation of the PV model	Simulation of the PV model	Absolute error (%)
$P_{MPP}$ (W)	783.0770	772.9946	1.2875	636.8692	620.1218	2.6296
$V_{MPP}$ (V)	78.8351	78.8296	0.0070	74.6604	74.6396	0.0279
$I_{MPP}$ (A)	9.9331	9.8059	1.2806	8.5302	8.3082	2.6025
$V_{OC}$ (V)	92.9164	91.9056	1.0879	86.9409	86.0016	1.0804
$I_{SC}$ (A)	13.9305	13.9500	0.1400	11.9426	11.9697	0.2269



manufacturer) of PV modules, having any number of bypass diodes and for any shading pattern (irradiance and temperature), by simply inputting in the program code, the values of the parameters of PV module specified in the datasheets supplied by the manufacturers. The program code of the proposed modelling can be implemented by any software tool according to the utility requirements. The proposed modelling of PV array is implemented using MATLAB programming in this paper and the corresponding results and output curves are validated respectively with the results generated by MATLAB simulation and data produced by the experimental procedure. The validation of the proposed modelling has been accomplished for five test cases subjected to two different PV arrays. The validation process ensured that the proposed equations produce correct results and hence can be employed for the planning and implementation of the practical operations involving PV devices. The proposed method is proved to be superior to the simulation method because of the former's potential to accurately forecast the output of the large-scale PV arrays within seconds and thus saving the designing and processing time to a great extent.

### List of symbols

$G$	Irradiance ( $\text{W/m}^2$ )
$T$	Temperature of the PV module (K)
$I_{pv}$	Photovoltaic current of the PV module (A)
$I_0$	Reverse saturation or leakage current of the PV module (A)
$a$	Diode ideality constant of the PV module
$R_s$	Equivalent series resistance of the PV module ( $\Omega$ )
$R_p$	Equivalent parallel resistance of the PV module ( $\Omega$ )
$V_t$	Thermal voltage of the PV module (V)
$N_s$	Number of cells connected in series in the PV module
$q$	Electron charge ( $1.60217646 \times 10^{-19}$ C)
$k$	Boltzmann constant ( $1.3806503 \times 10^{-23}$ J/K)
$V_{oc}$	Open-circuit voltage of the PV module (V)
$I_{sc}$	Short-circuit current of the PV module (A)
$K_{V_{oc}}^G$	Irradiance coefficient of $V_{oc}$
$K_{V_{oc}}^T$	Temperature coefficient of $V_{oc}$ (V/K)
$K_{I_{sc}}^T$	Temperature coefficient of $I_{sc}$ (A/K)
STC	Standard test condition ( $G = 1000 \text{ W/m}^2$ and $T = 25^\circ\text{C}$ )

### Declarations

**Conflict of interest** On behalf of all authors, the corresponding author states that there is no conflict of interest.

### References

- [1] Shah R, Mithulananthan N, Bansal R C and Ramachandaramurthy V K 2015 A review of key power system stability challenges for large-scale PV integration. *Renewable and Sustainable Energy Reviews*. 41: 1423–1436
- [2] Fan Y, Wang P, Heidari A A, Chen H, Turabieh H, Mafarja M 2022 Random reselection particle swarm optimization for optimal design of solar photovoltaic modules. *Energy*. 239: 121865
- [3] Pachauri R K, Kansal I, Babu T S and Alhelou H H 2021 Power losses reduction of solar PV systems under partial shading conditions using re-allocation of PV module-fixed electrical connections. *IEEE Access*. 9: 94789–94812
- [4] Patel H and Agarwal V 2008 MATLAB-based modeling to study the effects of partial shading on PV array characteristics. *IEEE Transactions on Energy Conversion*. 23: 302–310
- [5] Kreft W, Przenzak E, Filipowicz M 2021 Photovoltaic chain operation analysis in condition of partial shading for systems with and without bypass diodes. *Optik*. 247: 167840
- [6] Belhachat F and Larbes C 2015 Modeling, analysis and comparison of solar photovoltaic array configurations under partial shading conditions. *Solar Energy*. 120: 399–418
- [7] Sharma S, Varshney L, Elavarasan R M, Vardhan A S S, Vardhan A S S, Saket R K, Subramaniam U and Hossain E 2021 Performance enhancement of PV system configurations under partial shading conditions using MS method. *IEEE Access*. 9: 56630–56644.
- [8] Ahmada R, Murtazaa A F, Sherb H A, Shamic U T and Olalekand S 2017 An analytical approach to study partial shading effects on PV array supported by literature. *Renewable and Sustainable Energy Reviews*. 74: 721–732
- [9] Abdulmawjood K, Alsadi S, Refaat S S and Morsi W G 2022 Characteristic study of solar photovoltaic array under different partial shading conditions. *IEEE Access*. 10: 6856–6866
- [10] Jha V and Triar U S 2019 A detailed comparative analysis of different photovoltaic array configurations under partial shading conditions. *International Transactions on Electrical Energy Systems*. 29: e12020
- [11] Bai J, Cao Y, Hao Y, Zhang Z, Liu S and Cao F 2015 Characteristic output of PV systems under partial shading or mismatch conditions. *Solar Energy*. 112: 41–54
- [12] Daliento S, Napoli F D, Guerriero P and d'Alessandro V 2016 A modified bypass circuit for improved hot spot reliability of solar panels subject to partial shading. *Solar Energy*. 134: 211–218
- [13] Ko S W, Ju Y C, Hwang H M, So J H, Jung Y-S, Song H-J, Song H-e, Kim S-H and Kang G H 2017 Electric and thermal characteristics of photovoltaic modules under partial shading and with a damaged bypass diode. *Energy*. 128: 232–243
- [14] Ramabadran R and Mathur B L 2012 A comprehensive review and analysis of solar photovoltaic array configurations under partial shaded conditions. *Int. J. Photo Energy*. 2012: 1–16
- [15] Jha V and Triar U S 2017 An improved generalized method for evaluation of parameters, modeling, and simulation of photovoltaic modules. *International Journal of Photoenergy*. 2017: 1–19